Developing an Algorithm for Urban Flood Management With the Aim of Reducing Damage and Costs Using the Concept of Conditional Value at Risk

Pedram Eshaghieh Firoozabadi
Islamic Azad University Science and Research Branch
sara nazif (snazif@ut.ac.ir)
University of Tehran
Seyed Abbas Hosseini
Islamic Azad University Science and Research Branch
Jafar Yazdi
Shahid Beheshti University

Research Article

Keywords: Urban flood, cellular automata (CA), overland flow simulation, Best management practice (BMP), Conditional value at risk (CVaR), flood depth-damage functions

Posted Date: March 6th, 2021

DOI: https://doi.org/10.21203/rs.3.rs-266864/v1

Developing an algorithm for urban flood management with the aim of reducing damage and costs using the concept of conditional value at risk

PEDRAM ESHAGHIEH FIROOZABADI, SARA NAZIF (Corresponding Author), SEYED ABBAS HOSSEINI, JAFAR YAZDI

Pedram Eshaghieh Firoozabadi, Department of Civil Engineering, Science and Research Branch, Islamic Azad University, Tehran, Iran, Email Address: pedram.eshaghieh@gmail.com

Sara Nazif (Corresponding Author), School of Civil Engineering, College of Engineering, University of Tehran, Iran, Email Address: snazif@ut.ac.ir

Seyed Abbas Hosseini, Department of Civil Engineering, Science and Research Branch, Islamic Azad University, Tehran, Iran, Email Address: abbas_hoseyni@srbiau.ac.ir

3Faculty of Civil, Water and Environmental Engineering, Shahid Beheshti University, Tehran, Iran, Email Address: j_yazdi@sbu.ac.ir

Abstract

Flooding in urban area affects the lives of people and could cause huge damages. In this study, a model is proposed for urban flood management with the aim of reducing the total costs. For this purpose, a hybrid model has been developed using SWMM and a quasi-two-dimensional model based on the cellular automata (CA) capable of considering surface flow infiltration. Based on the hybrid model outputs, the best management practices (BMPs) scenarios are proposed. In the next step, a damage estimation model has been developed using depth-damage curves. The amount of damage has been estimated for the scenarios in different rainfall return periods to obtain the damage and cost- probability functions. The conditional value at risk (CVaR) are estimated based on these functions which is the basis of decision making about the scenarios. The proposed model is examined in an urban catchment located in Tehran, Iran. In this study, five scenarios have been designed on the basis of different BMPs. It has been found that the scenario of permeable pavements has the

lowest risk. The proposed model enables the decision makers to choose the best scenario with the minimum cost taking into account the risk associated with each scenario.

Keywords: Urban flood; cellular automata (CA); overland flow simulation; Best management practice (BMP); Conditional value at risk (CVaR) ; flood depth-damage functions

Introduction

Flood, as one of the most important natural disasters, causes a lot of damage to the world communities every year. Due to the population density and consequently various infrastructures and uses, urban areas are more vulnerable to the damage. On the other hand, today with the expansion of cities to the large areas, most of which have low permeability and temporary depression storage, the amount of damage has increased dramatically. Hence, the importance of planning to reduce flood damage has been emphasized throughout the global community. Every year, many methods and tools are created and developed for the flood management purposes. These methods and tools alone or in a combinative form can be used as an effective solution to mitigate the flood damages. Many researches have been conducted in different parts of the world in order to increase the flood management ability, some of which are mentioned in the following.

The first necessary step in the researches related to the urban floods is to examine the current situation of the city in the face of possible floods. For this purpose, the behavior of the drainage system should be simulated and flood zone must be determined and necessary strategies should be considered in order to improve the performance according to the floods occurred in previous years and related return periods. Usually, modeling the urban flood flows in the urban drainage system and its outflow is conducted in one-dimensional (1D), two-dimensional (2D) or a combination of them, each has its own advantages and limitations. The 1D methods have been widely used for many years to simulate flow in urban drainage systems because they are relatively easy to adjust, calibrate and explain. However, these methods have limitations such as the inability to fully simulate the complex

interaction between flow in the surface water harvesting network and runoff outside the network in the urban area (Seyoum et al., 2012). The 2D flow modeling techniques have made it possible to simulate the flood more accurately, determine the implementation site of the flood controlling and damage reducing measures and also to simultaneously model the flow inside the drainage network and corresponding outflow. Due to the complexities of modeling, the use of 2D models requires far higher computational time and costs than the 1D ones. This issue has made the use of 2D models difficult and sometimes unaffordable for large areas.

Due to the simple adjustment, relatively easy calibration and high simulation speed in 1D models, as well as leading to good simulation results for the urban drainage network, one can use them to model the urban network flow and compensate the weakness in modeling the outflow through combining these models with a two-dimensional one.

One of the practical open source 1D models of the urban drainage system is the SWMM simulation model. This model is capable of simulating different mechanisms of runoff production for single events or a sequential rainfall event in the urban areas (Zhang and Pan, 2014). The SWMM software uses a 1D flow routing model in an urban drainage network, which is a combination of pipes and open channels. When the hydraulic gradient line is above the ground level, the excess flow overflows and water is discharged from the node to the ground. In this case, the SWMM model is unable to simulate the behavior of the discharged overflow from the node and thus does not consider it in the simulation. This is one of the major limitations of this model. To overcome this limitation, a 2D flow simulation model can be used to model the outflow from the nodes. Due to the large size and complexity of urban topography, the use of conventional hydraulic models such as TRIM2D (Transient Inundation 2-Dimensional) (Casulli, 1990) and TUFLOW (BMT WBM Machinery

73 Group, 2011) is difficult and very complex for simulating the overflow from the network and has its
74 own complexities. (Schmidt et al., 2004).

75 In order to overcome these limitations, the present study employs a quasi-2D CA-based model for
76 the 2D hydraulic modeling. The CA approach, as a mathematical modeling tool, has been developed
77 based on the cellular spaces (Chopard and Droz, 2005). Dottori and Todini (2011) developed an
78 urban flood simulation model based on the CA approach and compared the obtained results with
79 analytical solutions as well as some hydraulic models. They indicated the high capability of the
80 proposed CA-based model in simulating the flooded areas in flood events. Liu and Pender (2013)
81 presented a hydrodynamic model using CA approach in order to simulate the flood spreading in
82 Carlisle, England. Their findings showed an agreement between the results of the proposed method
83 and the measured data during flood events. Cirbus and Podhoranyi (2013) employed the CA method
84 to simulate the complex process of water flow at the ground level. They introduced simple rules and
85 conditions that affect the water movement, including the slope, infiltration and roughness as the
86 inputs to the CA model. The obtained results showed that the CA method requires less computational
87 time to model the flow than other ones, which use 2D flow motion equations. Using the CA theory,
88 Jamali et al. (2019) modelled floods in urban areas and compared the results with those via 2D ones.
89 This comparison illustrated that the proposed CA-based model results in higher flood wave speed
90 than the 2D models. It has also been able to predict flooded area and flood depth with acceptable
91 accuracy.

92 Most of developed 2D models have only simulated the outflow from the rivers, flood channels or
93 urban drainage network. However, they are not able to consider solutions in order to reduce the
94 volume of flood outflow from the network. In the meantime, few investigations have addressed this
95 issue such as the study conducted by Abbasizadeh et al. (2017). They proposed a quasi-2D model

based on the CA theory. Connecting this model to the SWMM software, they were able to detect the nodes from which the water is outflowed, along with the hydrograph of the outflows and simulate those, which flow in two dimensions. This model is able to return the outflow from the node to the network in places where there is excess capacity. Tavakolifar et al. (2021) made some improvements in CA part of the model developed by Abbasizadeh et al. (2017) to improve the solutions stability. Among the shortcomings of flow simulation models in the studies conducted by Tavakolifar et al. (2021), Abbasizadeh et al. (2017) and Jamali et al. (2019), one can mention the inability of these models in modeling the effects of permeability of the study area at the flood volume and flow simulation. This makes these models not capable of modeling changes in the flow status and permeability amount of catchment due to the use of BMPs.

BMPs are modern urban runoff management technologies, which aim to restore the natural conditions of the catchment being destructed through urban development. Perez-Pedini et al. (2005) and Karamouz and Nazif (2013) attempted to control the urban flood using methods based on the permeability. They extracted the optimal location and number of infiltration-based BMPs in order to reduce the maximum amount of flood in the urban catchment area using a hydrological model and genetic algorithm. Using three evolutionary multi-objective algorithms of NSGA-II, NSHS and MOPSO in combination with SWMM software, Yazdi et al. (2015) developed a method for presenting optimal designs in the buried storm water network.

Various studies have been conducted on the BMP diversity and their influences on the urban runoff (Jia et al., 2013; Walsh et al., 2014; Moura et al., 2016 and Aminjavaheri and Nazif, 2018) all of which point out the ability of BMPs in reducing the flooding. In particular, the infiltration-based BMPs can be considered as an appropriate option for the urban floods due to the economic reasons

and high land use density. Therefore, there is a need for a model capable of modeling the infiltration-based BMPs through considering the effect of infiltration in flood simulation.

However, due to very high uncertainties in the urban runoff management issues, in order to determine the effectiveness of a policy, the existing uncertainties in the response of the policy should be considered in its evaluation. For this purpose, an attempt has been made to consider these uncertainties and their associate risks in making decisions about the selection of appropriate BMPs. For this purpose, CVaR approach is employed here. The concept of CVaR has been examined as a potentially effective tool for combining the possible uncertainties in water resources management. This method was first proposed by Artzner et al. (1999) and developed by Anderson and Uryasev (1999) and Rockafellar and Uryasev (1999, 2002). Also, CVaR has been employed to measure and optimize the expected risk from severe damage with lower probabilities (high loss). CVaR metric has been widely used in financial problems (Filippi et al., 2017). However, its applications have so far been limited in the context of flood-related areas. CVaR has been used in reservoir operation issues in order to minimize the environmental damage due to declining water levels (Webby et al., 2007; Yazdi et al., 2015). Compared to the scenario analysis approaches, CVaR has been shown to provide more reasonable cost estimates and better control over high-risk losses in issues associated with the water resource management (Yamout et al., 2007).

In the current study, in order to develop and improve the drainage system performance, a model is first developed for the simultaneous simulation of the drainage system and surface runoffs which its basis is taken from Tavakolifar et al. (2021). Tavakolifar et al. (2021) have not taken into account the infiltration effect in two dimensions. The present study develops a quasi-2D model capable of simulating the infiltration in the surface flow routing, which allows for the possibility of reducing flood damage through using different infiltration-based BMPs in the study area. In addition to the

141 cost and damage, an important criterion for selecting the best flood management strategy is the
142 amount of the associated risk. For this purpose and to choose the best strategy with the minimum
143 expected risk, the CVaR method has been used. This different approach in selecting BMPs in urban
144 areas, which has been addressed for the first time in the current study, helps decision makers with
145 choosing the best scenario considering the risk of damages caused by different rainfalls.

146 **Methodology**

147 As mentioned earlier, a flood management model has been developed in the present research with
148 the aim of reducing damage and costs using the concept of CVaR. The research has been conducted
149 according to the following steps (Figure 1):

150 1. Determining the design rainfall with different return periods and its hyetograph
151 2. Developing a quasi-2D hybrid model considering the flow permeability in order to simulate
152 the flow in drainage channels and also over the ground surface. This model simulates the
153 flow in the urban drainage system (UDS), which leads to the determination of its flow
154 characteristics and calculation of the hydrographs of the outflows from the manholes in the
155 study area. This model is capable of modeling the network outflow in a quasi-2D manner
156 along with specifying the flooding depth and range, taking the effect of infiltration into
157 account.
158 3. Determining the flooding locations and their characteristics in different parts of the city
159 4. Determining the type, location and dimensions of possible BMPs that can be used in the
160 region and defining their implementation scenarios
161 5. Developing a damage estimation model based on the inundation depth
162 6. Developing the damage-probability curve for each runoff management scenario considering
163 rainfalls with various return periods

7. Calculating CVaR at different confidence levels for each scenario
8. Determining the best scenario for the city runoff management

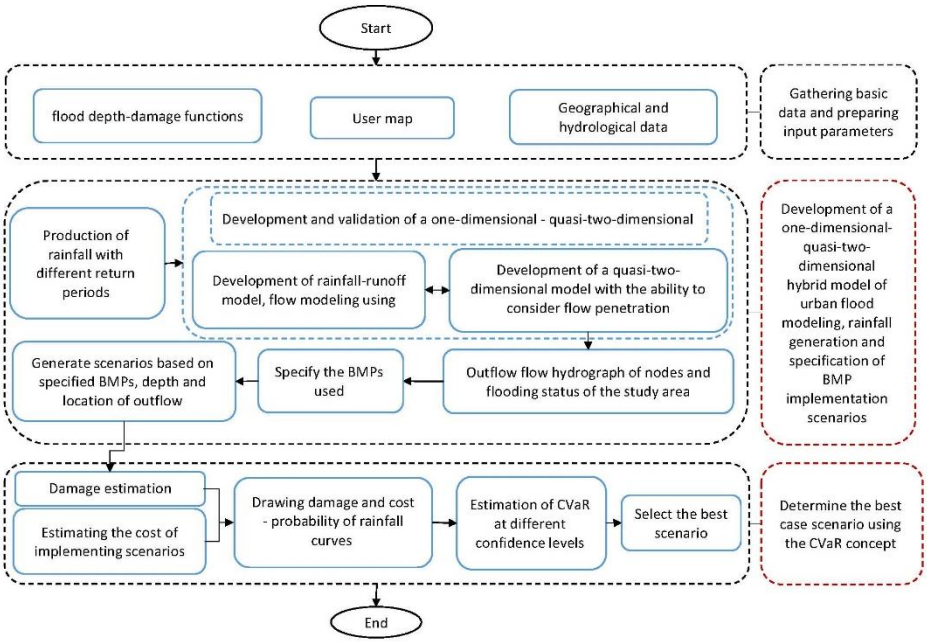

Figure 1. The proposed flood management algorithm with the aim of reducing the damage and cost using the concept of CVaR

1. 1D-quasi-2D urban flood simulation model considering the infiltration

In this section, it is attempted to make a connection between the SWMM and the developed CA-based 2D models in order to develop a quasi-2D model for the urban runoff simulation. In the CA section, the infiltration modeling capability has been also considered. The structures of these models are described in the following.

1.1. Urban runoff simulation in the 1D-quasi-2D model

Using SWMM model, the amount of runoff produced at the output point of each sub-catchment is calculated and considered as the urban drainage system (UDS) inlet flow. Then, the 1D flow routing is carried out in the UDS and flow characteristics such as flow depth and discharge rate are

178 determined along the channels and pipes in different time steps. During the simulation, when the
179 hydraulic gradient line is above the ground level, the hydrographs associated with the manhole
180 outputs are determined based on the outflow (Seyoum et al., 2012). This excess flow causes flooding
181 in the areas around the manhole, especially the downstream.

182 The hydrographs of the manhole outflows, determined by SWMM simulation, are used as input
183 data for the quasi-2D model. The quasi-2D model simulates the overflow of manholes that run
184 through the streets of the catchment. During the flow simulation, when the surface flow reaches a
185 node from which there is no outflow (manhole), part of it enters the system until reaching the full
186 UDS capacity. The inlet flow hydrograph is then determined using the quasi-2D model. In this case,
187 the UDS function is simulated again by means of SWMM. If the re-entry of surface flow into the
188 UDS causes outflowing from the downstream manholes, the quasi-2D model will run again. This
189 process continues until all the effects of these two flows are considered. In this research, the CA
190 theory has been used to develop the quasi-2D model.

191 **1.2. Flow modeling process in the quasi-2D model based on CA theory**

192 CA is a mathematical model which uses only local rules instead of complex differential equations in
193 order to model the behavior of physical systems. This approach uses simple neighborhood rules in
194 the modeling process even for the complex systems. To simulate the surface flow (flood) behavior
195 using CA, the study area is meshed using a square grid. Then, the water movement in each time step
196 is simulated in the following order:

197 1) Identifying cells with considerable infiltration because of BMPs implementation and introducing
198 the characteristics of infiltration equation to them.

199 2) Determining the flow path in each cell by comparing the water level in the target cells and their
200 neighbors.

3) Calculating the volume of inflow to and outflow from each cell in both directions.

4) Calculating the amount of infiltration within the implementation area of infiltration-based BMPs and return water to the manhole.

5) Calculating the volume and depth of water in each cell in a time step using continuity equation and the flows obtained in the previous time step.

6) Continuing the process from step 2 to the end of the time steps.

In this study, the equations proposed by Dottori and Todini (2010) have been used to calculate the flow between cells (Eq. (1)).

$$Q_{ij} = \frac{b h_m^{5/3}}{n} \left(\frac{H_i - H_j}{\Delta \mathcal{X}}\right)^{1/2} \quad (1)$$

Here, H_i and H_j are the heights of water in two neighboring cells (m), b is the cell width (m) and $\Delta \mathcal{X}$ stands for the distance between the centers of two adjacent cells (m). Furthermore, h_m describes the average water height in two neighboring cells (m), n is the Manning's roughness coefficient and Q_{ij} denotes the water flow rate displaced between the two adjacent cells. In this study, the von Neumann neighborhood method has been used for flow exchanging with four neighboring cells in the up, down, left and right directions as shown in Figure 2.

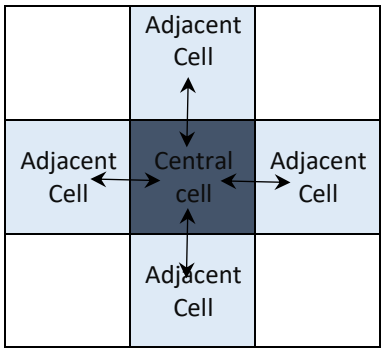

Figure 2. The use of von Neumann neighborhood method to connect the cells

Since each cell is only affected by four neighboring cells in two directions, the governing equations are separately solved for each direction. In the developed scheme, the current state of the system depends on the previous time step, so the computational approach is explicit. After estimating the flow displacement between cells by Eq. (1), the change in water volume per cell is obtained from the following relationship

$$Q(V_i) = \frac{\Delta V_i}{\Delta t} = \sum_{j=1}^{m=4} Q_{ij} \quad (2)$$

where V_i is the volume of water inside the *i*th cell (m^3) and Δt stands for the time step (s).

In order to accurately model infiltration-based BMPs, it is necessary to simulate the amount of infiltrated flow in the surface flow simulations. In order to consider the infiltration in the development of the quasi-2D model, one can determine the amount of infiltration in each time step per cell and subtract from the volume of water inside the cell. Due to the widespread use in similar studies such as McClymont (2007) and Clemmens et al. (2003) and ease of estimating the coefficients, the Kostiakov equation was used here to estimate the infiltration as in Eq. (3).

$$Z = kt^a \quad (3)$$

In the above equation, *a* (dimensionless) and k (m^3/m/min) are the experimental parameters corresponding to the type of surface material. Since the amount of infiltration is cumulative, in order to obtain the infiltration value in each time step, the derivative of Eq. (3) must be obtained with respect to time. As a result, the infiltration rate in each time step is achieved as given by Eq. (4).

$$z=k.a.t^{(a-1)} \quad (4)$$

Using Eq. (4) in each time step, the amount of infiltration in each cell is calculated and subtracted from the volume of water inside it while correcting the return flow to the manholes. Using Eqs. (5) and (6), the water volume and height in the cell are updated in each time step.

$$\Delta V_{t+\Delta t} = \Delta t.\, Q(V_t) + O(Q^2) + z \quad (5)$$

$$h_i = \frac{V_i}{dx.dy} \quad (6)$$

Here, h_i is the water depth in the cell (m), dx and dy denote the mesh dimensions in the x and y directions (m), respectively, z is the water infiltration height in the cell (m) and $O(Q^2)$ stands for the amount of water returning from the cell to the manhole.

2. Identification of the BMPs used in the modeling

The infiltration-based BMPs usually do not require free urban space and are less likely to affect the urban land uses. Therefore, they can be widely employed to reduce the effects of flooding and complete the urban drainage network. Another type of BMP which can be established inside the green marginal spaces along highways and does not require land possession is concrete reservoirs that are used as a BMP type. According to the above-mentioned points, in this study, the permeable asphalt, permeable pavement, vegetative Swale and local concrete reservoirs with low capacity have been used.

3. Damage estimation

In general, the flood-induced damages can be divided into direct and indirect categories. The direct damages are caused because of inundation impacts on infrastructures and properties (Karbasi et al., 2019) while indirect damages occur after the direct ones and are considered as the negative effects of them. The flood management is generally performed on the direct damages that are tangible and according to the relationship between the two types of damages, if direct damages are reduced, the indirect ones are also reduced. For this reason, the direct damages have been evaluated in the current research.

In this study, the corresponding diagrams presented in Joint Research Centre (JRC) technical reports have been used for developing depth-damage curves (Huizinga et al., 2017). In 2017, JRC presented a globally compatible database of flood depth-damage curves. This database includes the damage curves indicating the relative damages (%) as a function of water depth as well as the maximum amount of damage related to the various types of assets and land use classifications. The maximum amount of damage for each country has been specifically estimated according to the conditions of that country. For countries without these statistics, a fixed set of maximum flood damage values has been calculated using statistical regressions with global economic development indicators (Huizinga et al., 2017). For damage estimation, in the first step, the land use map is prepared in the geographic information system (GIS). In the next step, according to the depth-damage curve extracted from JRC technical reports, the amount of damage in each cell is determined corresponding to the type of specified land use and maximum water height. Finally, the damage to the whole area is estimated by aggregating the damages of each cell.

4. Conditional value at risk (CVaR)

Among the risk-based methods in the field of decision-making VaR and CVaR metrics are well-known techniques based on measuring the damage to the system. Figure 3 depicts the VaR and CVaR descriptions using probability density function of system loss. VaR is the probable damage amount at 1-α confidence level. In addition, the value of CVaR is equal to the mean of damages greater than VaR at the determined confidence level.

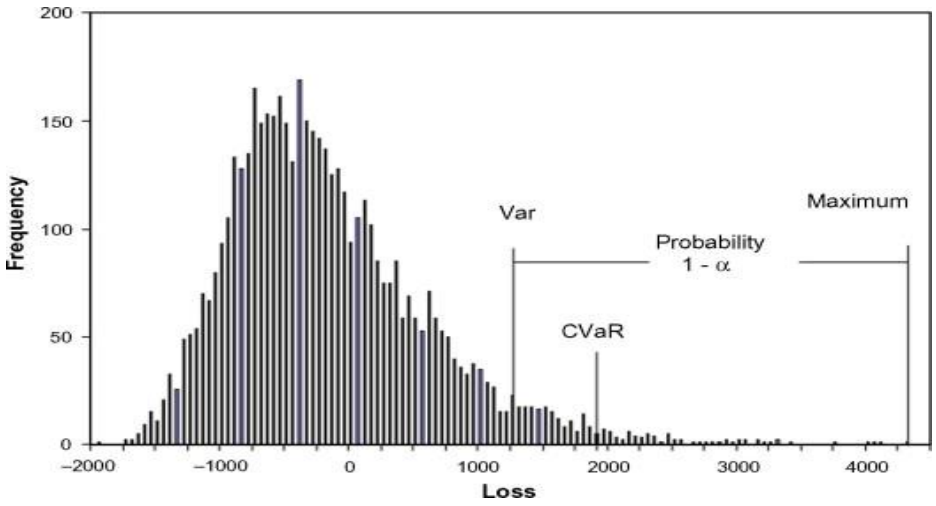

Figure 3. VaR and CVaR descriptions using damage probability density function (Rockafellar and Uryasev, 1999)

Assuming that $f(x,y)$ is the damage function in terms of the decision variable x and random variable y and $p(y)$ is the probability density function of y, the probability that f does not exceed a certain threshold α can be determined from Eq. (7). It should be noted that this probability for a constant value of x is the same as the distribution of losses (Rockafellar and Uryasev, 1999).

$$\psi(x,\alpha) = \int_{f(x,y)\leq\alpha} p(y)dy \tag{7}$$

If the values of VaR and CVaR for the damage function f and confidence level β are denoted by $\alpha_\beta(x)$ and $\varphi_\beta(x)$, respectively, it results in:

$$\alpha_\beta(x) = min\{\alpha\epsilon R : \psi(x,\alpha) \geq \beta\} \tag{8}$$

$$\phi_\beta(x) = (1-\beta)^{-1} \int_{f(x,y)\geq\alpha_\beta(x)} f(x,y)p(y)dy \tag{9}$$

According to the concept of CVaR, the lower the value of this measure, the lower the risk. In other words, the scenario having the lowest CVaR at the corresponding confidence level meets the most reliable performance and therefore can be selected as the best one.

Case Study

The developed hybrid model has been applied to select the best urban runoff management options in a case study located in Tehran, Iran. Tehran is located at longitude 51º 8′-57º 37′ and latitude 35º 34′-35º 50′. The altitude of Tehran varies between 1850 m in the north and 1100 m in the south. Tehran is surrounded by Shahriar and Varamin plains from the south and Alborz Mountains from the north (Nazif, 2011). The study zone is located in the northwestern part of Tehran with an area of 1010 ha. This zone includes mountainous and urban areas. The drainage system of this area includes main and secondary channels, most of which are concrete. The common land use types in this area are residential, commercial, pedestrian, industrial, green and office spaces. The location of the study area on the map is shown in Figure 4 together with the drainage system layout. The study area is faced with the flooding problem in the case of heavy rainfall in some locations, which causes traffic slowness or road closures and damage to some urban infrastructure such as electricity network, sewage and telecommunications.

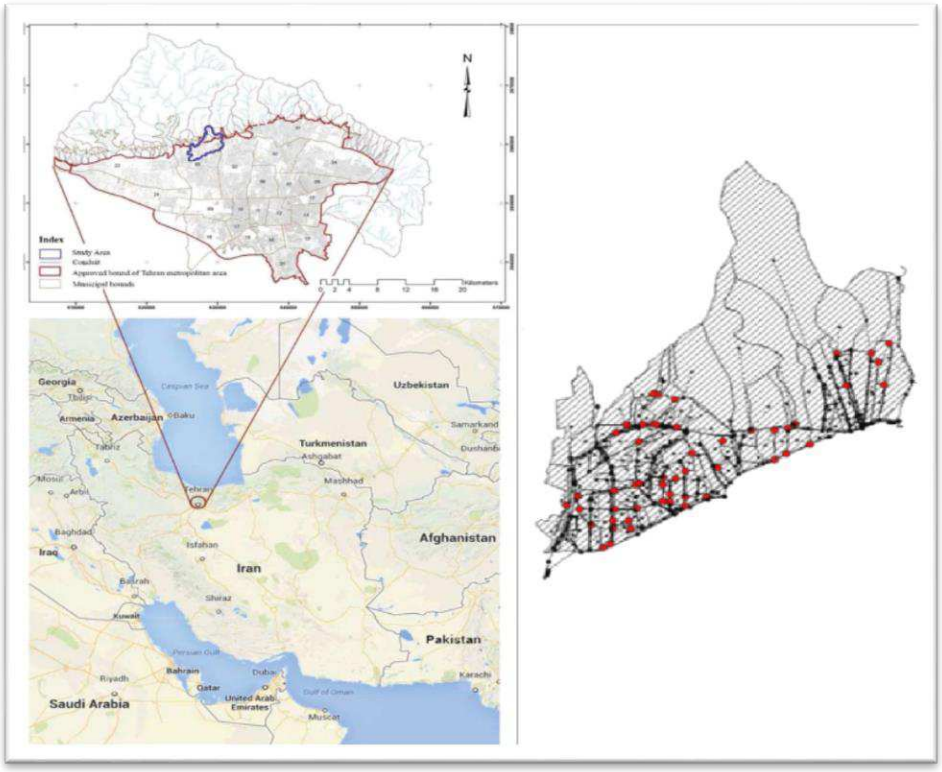

Figure 4. Location of the study area and general outline of the surface water harvesting network along with sub-catchments in the SWMM program

The catchment zoning in the mountainous areas has been done according to the digital elevation model (DEM) data. In urban areas, the service sub-catchment of channels has been determined using layers of 1:1000 urban maps and pavements grading (Mahab, G., 2011). The hydrological characteristics of the sub-catchments have been estimated using land use layers and location of the channels in each of them (Mahab, G., 2011). Table 1 presents the specifications of the study area.

Table 1. General specifications of the initial model of the case study area in SWMM software

Parameter or variable	Value or description	Unit
Total area of the modeled catchments	1010	ha
Average annual rainfall in Tehran	245	mm
Entire length of the modeled waterways network	58173	m

Range of the curve number associated with the sub-catchments (CN) (Mahab, G. ,2011)	70-86	--
Number of sub-catchments	141	--
Land use	Urban and mountainous	--
Medium slope range of mountainous catchments	27-45	%
Medium slope range of urban catchments	5.2-18	%
Type of channels	Circular and rectangular	--
Material of the channels	Concrete and polyethylene	--

Results and discussion

1. Validation of the developed quasi-2D model

In order to evaluate the accuracy of the developed quasi-2D model, the simulation results of a case study conducted by Clemmens et al. (2003) have been used. Clemmens et al. (2003) developed a 2D flow model taking the infiltration into account using shallow unsteady flow equations and Kostiakov infiltration equations. They used field data obtained by Strelkoff et al. (2003) to control the accuracy of their model. The study area was a 2.9-ha rectangular field with dimensions of 144*202.5 m and a slope of 0% whose soil type is sandy loam. The water inlet is approximately at the midpoint of the northern edge side (202.5 m). A road of 80 m length and 6 m wide extends into the ground from the southern edge.

The water level has been measured at 26 locations within the catchment. The farm plan and measurement stations are exhibited in Figure 5. The field's surface roughness coefficient is equal to 0.05 and the coefficients of Kostiakov infiltration equation for this field are reported by Clemmens et al. (2003) to be k=39 mm/ha and a=0.37. The inlet water flow to the farm is also variable and is described in Table 2.

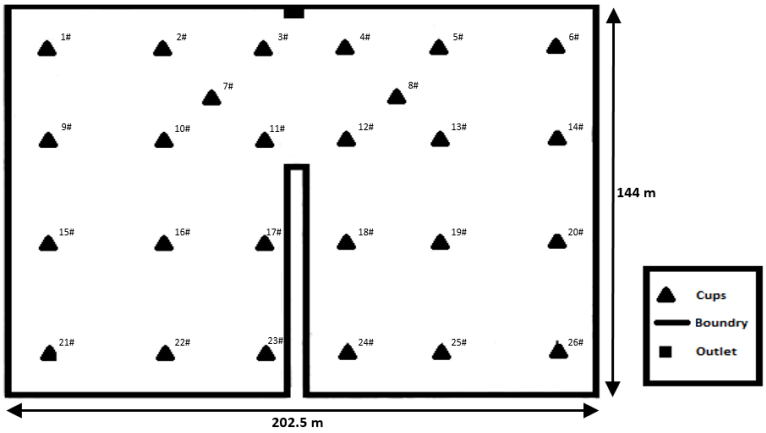

Figure 5. Layout for 2.9 ha Field

Table 2. The hydrograph of the inflow to the field

Time (min)	Flow rate (m^3/s)
0	0.419
4	0.411
14	0.411
22	0.419
59	0.450
74	0.462
84	0.470
90	0.470
97	0.470

According to the above-mentioned specifications, the flow modeling was carried out and the results are presented in Figures 6 and 7. Figure 6 presents the flow intrusions over time (min) associated with the field measurement, modeling results performed by Clemmens et al. (2003) and those via the quasi-2D CA model. As shown in this figure, the flow modeling via 2D CA model has led to acceptable results with a maximum error of 4.48% for the area covered. The area covered with respect to the time measured and calculated by the quasi-2D CA model is presented in Table 3.

348 **Table 3.** Advance times and area covered

Advance time (min)	Area covered (%) (Measured)	Area covered (%) (Simulated 2D CA)	Error (%)
15	26	27	3.70
30	47	48.7	3.49
45	67	68.7	2.47
60	81	84.8	4.48
75	94	97	3.09
90	99	100	1

349

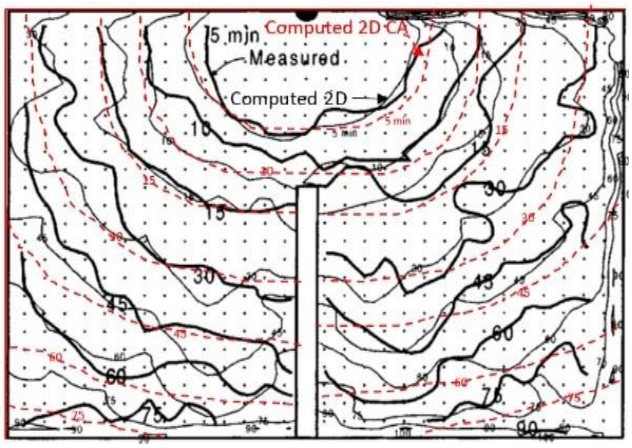

350

351 **Figure 6**. Flow intrusion lines associated with the field measurement, flow modeling conducted by

352 Clemmens et al. (2003) and flow modeling using quasi-2D CA model

353 Figure 10 displays the water level hydrographs corresponding to the measurements, 2D
354 simulations using shallow water equations and quasi-2D CA model for the stations 4, 8, 13 and
355 20. The water depth near the outlet is higher than the other parts of the field (station 4) which has
356 caused a high hydraulic gradient of the flow at that station. This makes it difficult to accurately
357 calculate the flow depth at this point. Due to the dimensions of the mesh considered for the
358 calculations (2*2 m), high hydraulic gradient of the water surface at points close to the flow inlet
359 and also high flow velocity that causes the soil bed to move, especially over time when the bed
360 displacement reaches its maximum value, the flow depth at point 4 indicates a maximum error of
361 15%. The greater the distance from the inlet point, the smaller the difference between the depths

estimated by the quasi-2D CA model and the one measured in the field. After cutting off the flow in 97 min, the flow level decreases uniformly and all parts of the field, reach an identical depth.

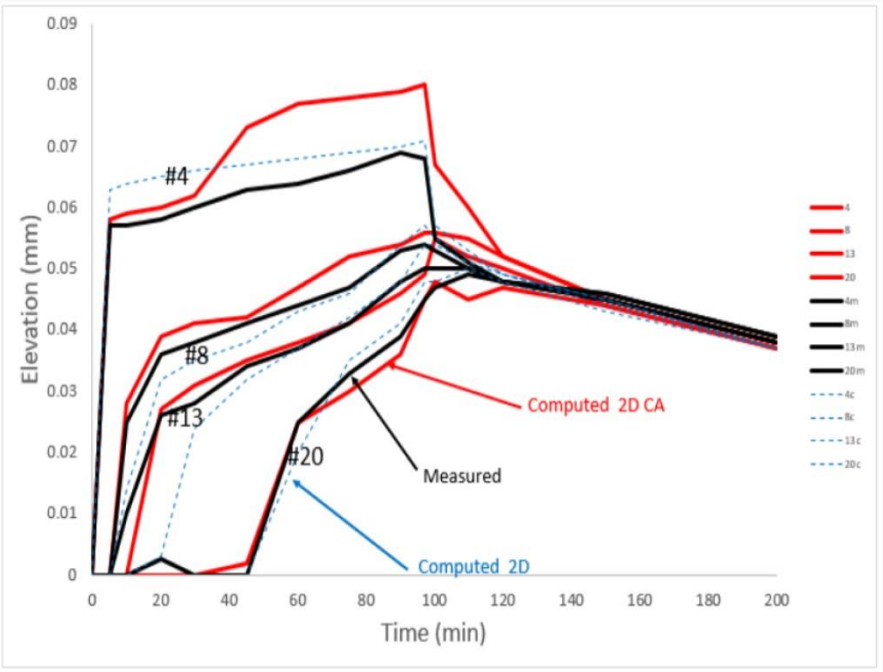

Figure 7. Flow hydrographs at points 4, 8, 13 and 20

5. Design rainfall with different return periods

In this research, in order to produce the precipitation with different return periods, the duration and hyetograph suggested in comprehensive plan of the surface waters management of Tehran (2011) has been used. The rainfall duration which causes the maximum flow in this region is the 6-hour precipitation (Mahab, G., 2011). Here, the precipitations with a return period of 5 to 200 years were used to generate the damage-probability function in order to increase the estimation accuracy of the CVaR value. The precipitation hyetographs for various return periods are given in Figure 8.

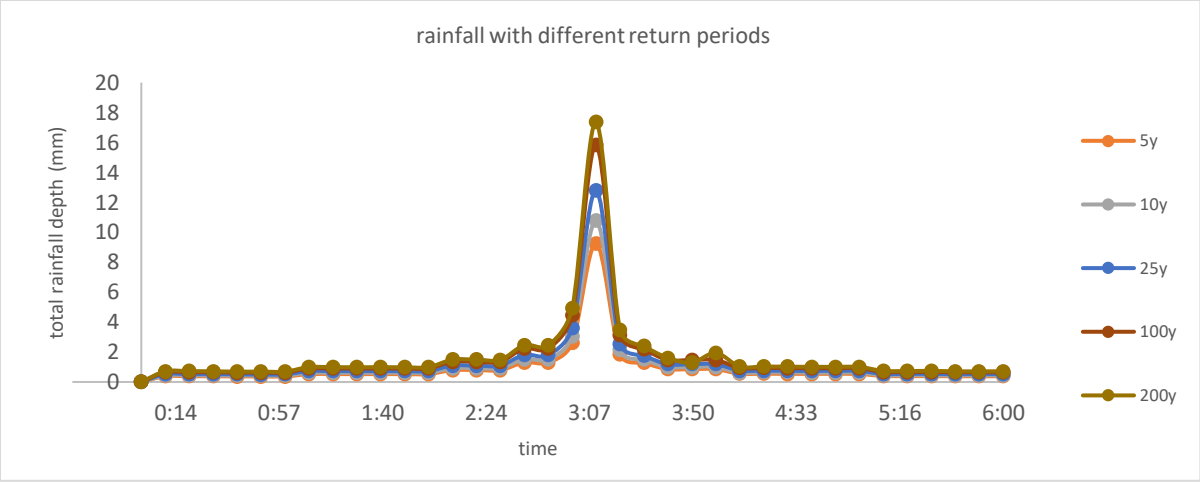

Figure 8. Design rainfall with different return periods for the study area

3. Flow simulation using developed 1D-Quasi-2D model

Considering the capabilities of the SWMM model, it is used for the rainfall-runoff simulation in this paper. The snowmelt ,evaporation, groundwater, and water quality components are neglected in this study. The Soil Conservation Service (SCS) curve number method is used for estimating precipitation losses as suggested in previous studies in Iran (Moghadamnia et al. 2015). Regarding the slope of the study area which is approximately high, and as the conduits are open channel, there is no flow reversal and pressurized flow in the drainage system, so the kinematic wave method is used for flow routing (Rossman 2010).

Table 2 presents the number of points in which overflowing from the network occurs along with the total outflow volume according to different rainfall return periods extracted from the SWMM model. The location of the outflow from the UDS for 10- and 100-year return periods is depicted in Figure 7. As would be observed, the number of overflowing points in the 100-year return period is more than twice the one corresponding to the 10-year period. In addition, as it can be seen in Table 4, the overflow volume from the total manholes has nearly quadrupled. The points from which the flow overflows are almost uniformly distributed over the study area, which can be seen

391 in Figure 9. The coordinates of the overflowing points along with the overflow hydrograph
392 resulting from the flow modeling in the UDS are entered the quasi-2D model.
393
394 **Table 4.** The number of points with overflowing and volume of the flow entering the quasi-2D model

Rainfall return period (year)	rainfall depth (mm)	Runoff volume ($10^3 \times m^3$)	Number flooded nodes	Volume of outflow from drainage network ($10^3 \times m^3$)
2	26.13	64	10	4
5	33.54	99	22	9
10	39.06	128	32	16
25	46.33	171	47	29
50	51.86	206	59	42
100	57.38	243	67	60
150	60.61	265	72	71
200	62.9	281	72	74

395

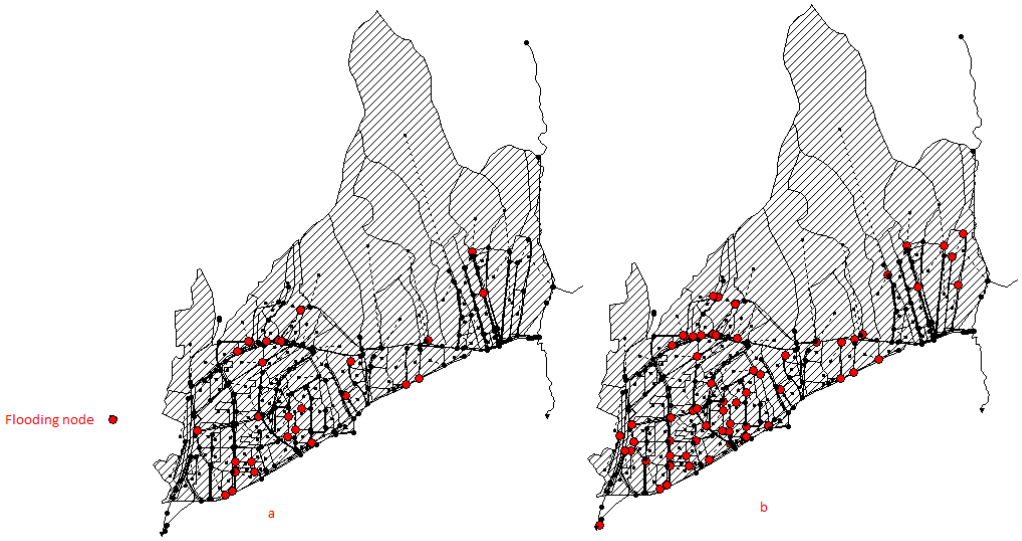

396
397 **Figure 9.** Node flooding for (a) 10-year and (b) 100-year return periods
398
399 **4. Selecting possible BMPs**
400 Due to the lack of space to implement various BMPs and high price of the land in the vicinity of
401 Tehran, in cases where network performance needs to be improved, BMPs that do not need new

space have been identified. In this study, the permeable pavement with permeable concrete surface, permeable asphalt, vegetative swale and small flood concrete reservoirs have been used, the cost of each is listed in Table 5.

Table 5. Specifications of the examined BMPs

BMP type	Implementation cost per unit (square meters-US dollars)
Permeable asphalt	15.7
Permeable pavement with permeable concrete surface	17.12
concrete reservoirs	210
Vegetative Swale	11.16

5. Implementation scenario of the BMPs

The outputs of the developed flood simulation model are the flooding sites along with the maximum occurred flooding depth. This information has been used to determine the implementation locations of the BMP scenarios and the corresponding area. In the study area, the surface water harvesting network has been designed for 50-year return periods and has been controlled for 100-year and 200-year ones. Therefore, the scenario design is performed based on the modeling results depicted in Figure 10. In the present study, each BMP implementation scenario only considers one type of BMP in order to better evaluate the performance of each BMP in each scenario. Thus, 5 different scenarios were specified, including: 1- Maintaining the current situation, 2- Using permeable asphalt which has a reservoir layer, with an area of 16 ha, 3- Using a permeable concrete layer which has a reservoir layer on pavements with an area of 4 ha, 4- vegetative swale with an area of 2.6 ha, 5- Using 4 concrete reservoirs of 1500 m^3 volume near to the manholes with a large volume of overflowing.

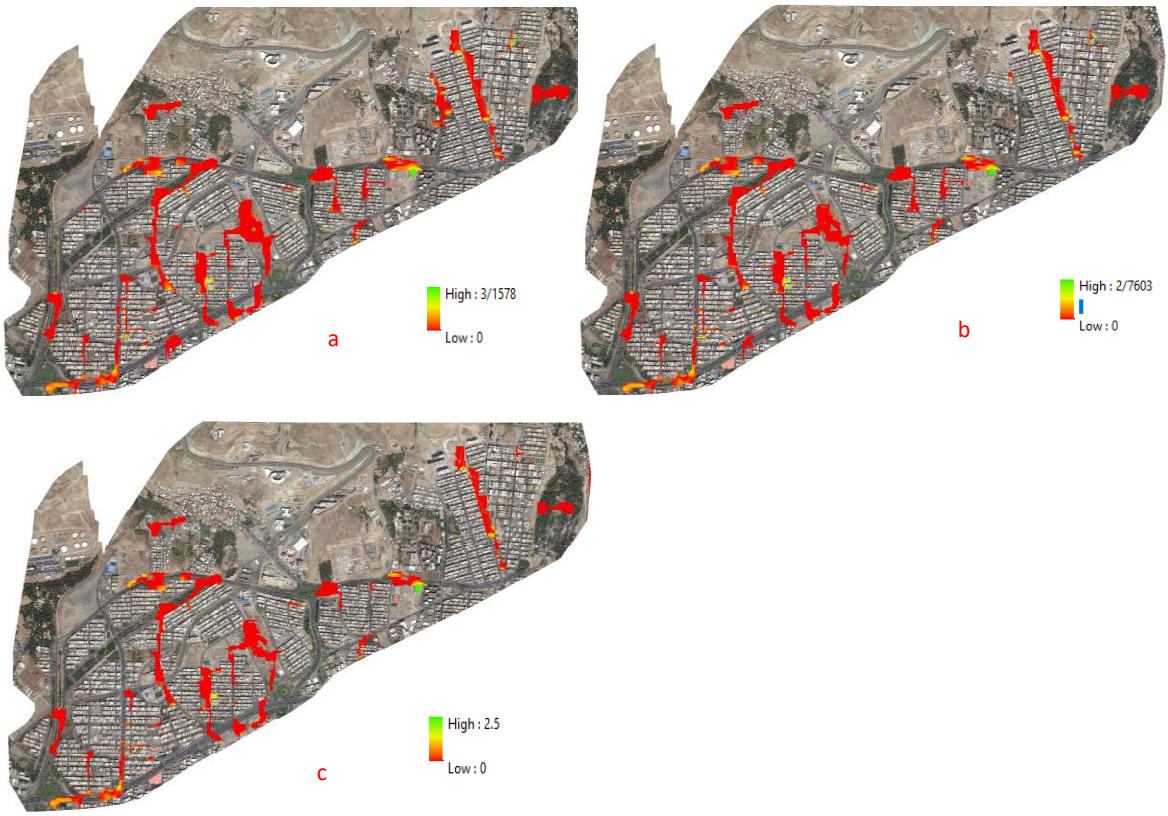

Figure 10. The modeled flooding range and depth associated with (a) 200-, (b) 100- and (c) 50-year return periods

6. Damage estimation

In order to estimate the damage, first, the urban land use maps are prepared in such a way to comply with the meshing used in the surface flow modelling. In the next step, using damage estimation functions extracted from JRC (2017), the amount of damage is estimated using the maximum flood depth and type of the land use assigned to the cell. The total damage is then estimated by aggregating the damage of all cells. This process has been separately performed in 5 scenarios for different rainfall return periods. The damage amounts are specified in Table 6 for different return periods and scenarios.

Table 6. Damage amount considering different BMP implementation scenarios and precipitation return periods

	Damage caused during the rainfall return period (million dollars)						Scenario implementation cost (million dollars)
Scenario	2 year	5 year	10 year	50 year	100 year	200 year	
1	0.49	1.36	3.10	6.36	8.48	10.07	0
2	0.13	0.47	0.87	1.89	2.84	4.64	2.5
3	0.13	0.48	1.24	3.87	5.36	7.37	0.7
4	0.50	0.99	2.48	6.05	8.17	10.39	0.3
5	0.27	1.14	2.07	4.97	8.06	10.32	0.4

435

436 **7. Damage and cost-precipitation probability curves**

437 To estimate the CVaR associated with each scenario, the amount of damage in each scenario is
438 estimated in different return periods and added to the corresponding implementation cost. Table 6
439 lists each scenario's implementation cost and damage in each return period. Using information in
440 Table 6, the damage and cost-probability curves are plotted in Figure 11 for different BMP
441 implementation scenario.

442 As shown in Figure 11, due to the zero cost in scenario 1, the damage and cost-probability curves
443 meet the lowest total amounts of damage and cost in the 2- and 5-year return periods. However,
444 increasing the return period, the damage increases with a much greater slope compared to other
445 scenarios, so that in the return period of 10 years onwards, the damage and cost meet their
446 maximum values. Due to the large initial implementation cost of scenario 2, its total cost and
447 damage up to the 10-year return period are more than all scenarios. However, after that, the total
448 damage and cost increase with a very small slope due to the high capacity of this scenario in
449 reducing the flood volume which leads to a better performance for floods with larger return periods
450 as a consequence. The other scenarios were found to have a function between scenarios 1 and 2.
451 As can be seen, each of the scenarios has advantages in different probabilities of occurrence, so a
452 criterion is needed to select the best scenario while comparing them.

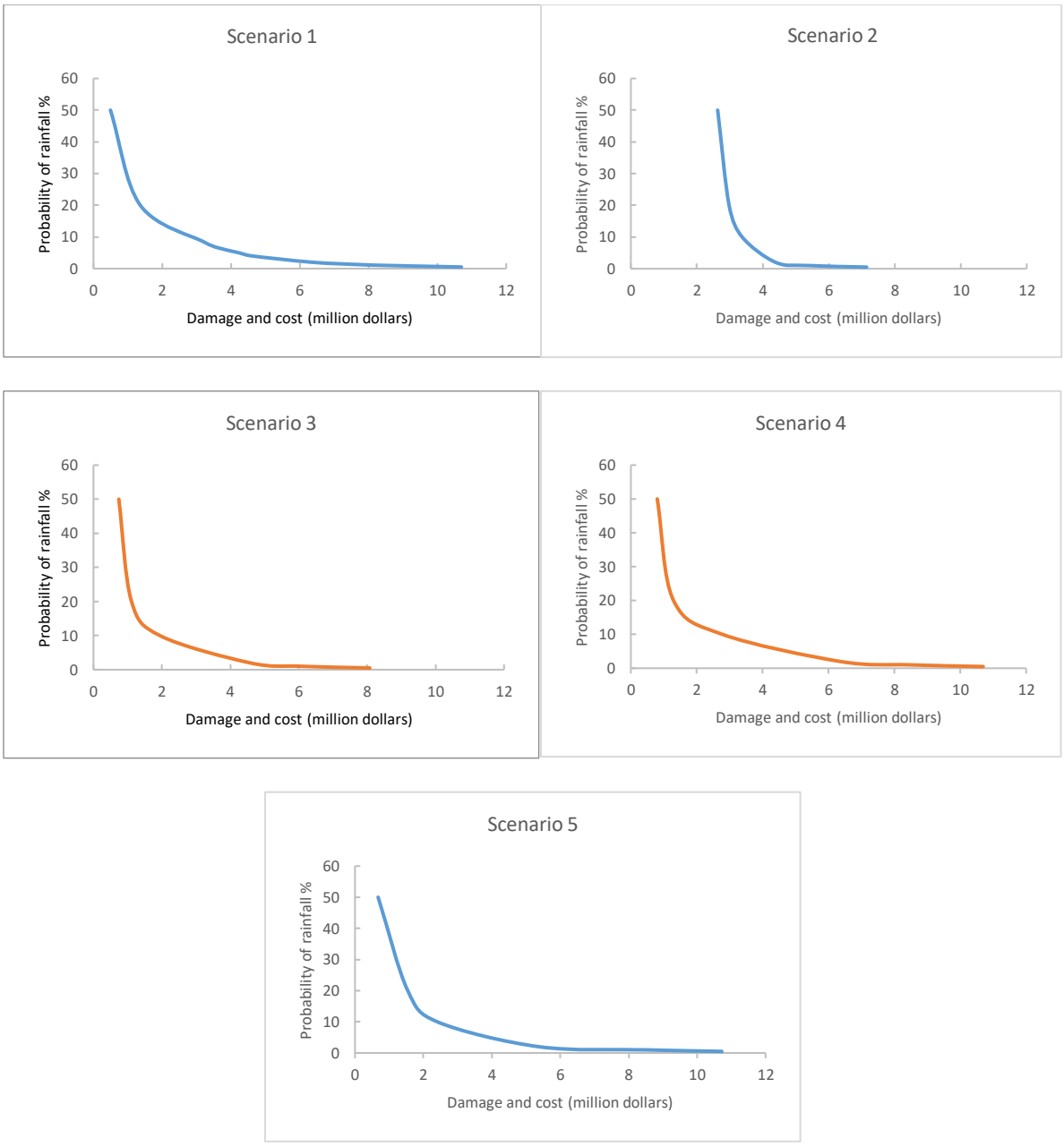

Figure 11. Damage versus probability for different scenarios

8. Determination of the best BMP implementation scenario

After plotting the cost and damage-probability curves for each scenario and comparing them, a criterion is needed to select the best scenario in terms of the performance. For this purpose, the CVaR method has been used in this research and three confidence levels of 95, 90 and 80% have

been calculated for each scenario. The calculated CVaR value for each scenario is given in Table 7 at the aforementioned confidence levels. As it is clear, scenario 3 has the lowest CVaR at all three confidence levels. To evaluate the overall performance of the scenario, the variation ranges of CVaR values are plotted in Figure 12 for different scenarios and confidence levels. As can be seen, the higher the damage reduction capacity in the scenarios, the smaller the CVaR variation ranges. In this regard, scenarios 2 and 3 had the best performances, respectively. Considering the implementation cost of the scenarios, scenario 3 has the lowest CVaR at the three confidence levels and can be generally selected as the best scenario.

Table 7. CVaR values at different confidence levels for the examined scenarios

Scenario	CVaR (million dollars)		
	confidence level 80%	confidence level 90%	confidence level 95%
1	3.57	5.1	6.45
2	3.87	4.27	4.86
3	2.79	3.36	4.6
4	3.47	4.94	6.15
5	3.82	4.78	5.9

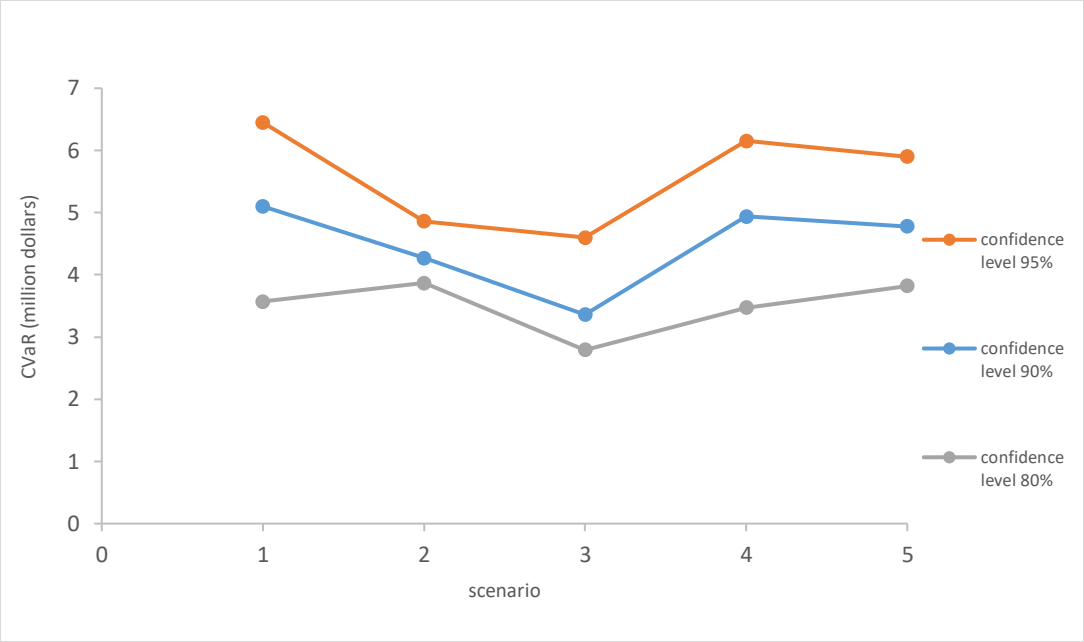

Figure 12. CVaR values at different confidence levels for various scenarios

Conclusion

In this research, the aim was to create a desirable flood management model in order to reduce damage and cost. To achieve these goals, the following steps have been taken. First, a 1D-quasi-2D model was developed to simulate the overflow and flow inside the drainage system considering the permeability. Then, according to the selected BMPs and the location and depth of flooding in the 50-year return period, the scenarios and their implementation sites were selected and controlled with 100- and 200-year periods. After this step, with the development of a damage estimation model, the amount of damage was estimated using the flood depth-damage function in different rainfall return periods and for different BMP implementation scenarios. According to the estimated implementation costs and damages associated with the scenarios, the cost and damage-probability functions were plotted for different scenarios. Finally, using cost and damage-probability diagrams, the value of CVaR was estimated at three different confidence levels. The quasi-2D CA-based modeling, in addition to increasing the computational speed, provides the researchers with

the location and maximum depth of flooding and also enables them to consider the exact implementation site of the scenarios. It should be mentioned that the scenarios which use infiltration-based BMPs, cannot completely eliminate the damage due to the gradual impact of these BMPs types. However, if the BMPs implementation is properly located and covered, they can effectively reduce the damage.

Another important aspect of this research is the examination of a new method in analyzing the damage and sustainability of different scenarios in urban floods. Due to the sensitivity of the CVaR concept to all probabilities of damage beyond the defined threshold, it can be considered as a reliable tool to help decision makers in choosing the superior scenario in the face of floods considering the two aspects of cost and damage. This concept plays an important role in choosing the best flood management approach. In this study, the CVaR values for permeable pavement were estimated as 2.79, 3.36 and 4.6 million dollars at three confidence levels of 80, 90 and 95%, respectively. According to the definition of CVaR, the lower the CVaR value, the lower the risk of damage caused by the implementation of that approach. The present findings indicated that the permeable pavement provides the best performance for this region among other strategies.

References

Abbasizadeh, H., Nazif, S., Hosseini, A. and Tavakolifar, H. (2017). Development of a coupled model for simulation of urban drainage process based on cellular automata approach. Irrigation and drainage, Published online in Wiley Online Library (wileyonlinelibrary.com). http://doi.org/10.1002/ird.2186

507 Aminjavaheri, S. M., & Nazif, S. (2018). Determining the robust optimal set of BMPs for urban
508 runoff management in data-poor catchments. Journal of Environmental Planning and
509 Management, http://doi.org/10.1080/09640568.2017.1337567
510 Andersson F and Uryasev S. (1999). Credit risk optimization with conditional value-at-risk
511 criterion. Research Report No. 99-9, University of Florida
512 Artzner P, Delbaen F, Eber JM, Heath D. (1999). Coherent measures of risk. Math Financ
513 9(3):203–228.
514 BMT WBM Machinery Group. (2011). https://www.bmtwbm.com
515 Cai X, Li Y, Guo X, Wu W. (2014). Mathematical model for flood routing based on cellular
516 automaton. Water Science and Engineering 7(2): 133–142. https://doi.org/10.3882/j.issn.1674-
517 2370.2014.02.002
518 Casulli, V. (1990). TRIM 2D (Transient Inundation 2-Dimensional Model). University of Trento:
519 Trento, Italy.
520 Chahar, B. R., D. Graillot, and S. Gaur. (2012). Storm-Water Management through Infiltration
521 Trenches. Journal of Irrigation and Drainage Engineering 138: 274–281.
522 https://doi.org/10.1061/(ASCE)IR.1943-4774.0000408
523 Chopard B, Droz M. (2005). Cellular Automata Modeling of Physical Systems. Cambridge
524 University Press: New York, USA. https://doi.org/10.1017/CBO9780511549755
525 Cirbus J, Podhoranyi M. (2013). Cellular automata for flow simulation on the earth surface,
526 optimization computation process. Applied Mathematics & Information Sciences 7(6): 2149–
527 2158. https://doi.org/10.12785/amis/070605

528 Clemmens, A. J., Strelkoff, T. S., and Playan, E. (2003). Field verification of two-dimensional
529 surface irrigation model. J. Irrig. Drain. Eng., 129(6), 402–411.
530 http://dx.doi.org/10.1061/(ASCE)0733-9437(2003)129:6(402)
531 Dottori F, Todini E. (2010). A 2D Flood inundation model based on cellular automata approach.
532 In Proceedings of International Conference on Water Resources, Cimne, Barcelona, Spain. June
533 21–24.
534 Dottori F, Todini E. (2011). Developments of a flood inundation model based on the cellular
535 automata approach: testing different methods to improve model performance. Physics and
536 Chemistry of the Earth 36: 266–280. https://doi.org/10.1016/j.pce.2011.02.004
537 Filippi C, Mansini R, Stevanato E. (2017). Mixed integer linear programming models for optimal
538 crop selection. Comput Oper Res 81:26– 39. https://doi.org/10.1016/j.cor.2016.12.004
539 Huizinga, H. J, de Moel, H & Szewczyk. (2017). W Global flood depth-damage functions.
540 Methodology and the database with guidelines. https://doi.org/10.2760/16510
541 Jamali, B., Bach, P. M., Cunningham, L., & Deletic, A. (2019). A Cellular Automata fast flood
542 evaluation (CA - ffé) model. Water Resources Research, 55, 4936–4953. https://doi.org/10.1029/
543 2018WR023679
544 Jia, H., H. Yao, and S. L. Yu. (2013). Advances in LID BMPs Research and Practices for Urban
545 Runoff Control in China. Frontiers of Environmental Science and Engineering 7 (5): 709–720.
546 https://doi.org/10.1007/s11783-013-0557-5
547 Karamouz M, Nazif S. (2013). Reliability-based flood management in urban watersheds
548 considering climate change impacts. Journal of Water Resources Planning and Management
549 139(5): 520–533. https://doi.org/10.1061/(ASCE)WR.1943-5452.0000345

550 Karbasi, M. Shokoohi, A. and Saghafian, B. (2019). Estimating Number of Fatalities Due to Flash
551 Floods in Residential Areas. Iran-Water Resources Research, 15(1), 150-160 (In Farsi)
552 Liu Y, Pender G. (2013). Carlisle 2005 urban flood event simulation using cellular automata-based
553 rapid flood spreading model. Soft Computing 17(1): 29–37. https://doi.org/10.1007/s00500-012-
554 0898-1
555 Mahab, G. (2011). Tehran Storm water Management Master Plan. (In Farsi) Tehran, Iran: Tehran
556 Engineering Technical Consulting Organization.
557 McClymont, D. (2007), Development of a decision support system for furrow and border
558 irrigation, PhD thesis. University of southern Queensland.
559 Moghadamnia, A., A. Sepahvand, M. Lashani Zand, and M. Rostami Khalaj. (2015). Application
560 of Artificial Neural Networks Technique to Infiltration Determination Based on SCS and
561 Kostiakov Models' Parameters. Desert Ecosystem Engineering Journal 4 (6): 77–86.
562 Moura, N. C. B., P. R. M. Pellegrino, and J. R. S. Martins. (2016). Best Management Practices as
563 an Alternative for Flood and Urban Storm Water Control in a Changing Climate. Journal of
564 Flood Risk Management 9 (3): 243–254. https://doi.org/10.1111/jfr3.12194
565 Nazif, S. (2011). Development of an Algorithm for Evaluation of Climate Change Impact on Urban
566 Water Cycle. PhD thesis. College of Engineering, School of Civil Engineering, University of
567 Tehran.
568 Perez-Pedini, C., Limbrunner, J. F., and Vogel, R. M. (2005). Optimal location of infiltration-
569 based best management practices for storm water management. Journal of Water Resources
570 Planning and Management, 131(6), 441-448. https://doi.org/10.1061/(ASCE)0733-
571 9496(2005)131:6(441)

572 Rockafellar RT, Uryasev S. (1999). Optimization of conditional value at risk. Journal of Risk
573 2:21–41.
574 Rockafellar RT, Uryasev S. (2002). Conditional value-at-risk for general loss distributions. J Bank
575 Financ 26:1443–1471. https://doi.org/10.1016/S0378-4266(02)00271-6
576 Rossman, L. A. (2010). Storm Water Management Model User's Manual Version 5.0. U.S.
577 Environmental Protection Agency, EPA/600/R-05/040. http://www2. epa.gov/water-
578 research/storm-water-management-model swmm#applications. Accessed June 26, 2015.
579 Schmit TG, Thomas M, Ettrich N. (2004). Analysis and modeling of flooding in urban drainage
580 systems. Journal of Hydrology 299: 300–311. https://doi.org/10.1016/j.jhydrol.2004.08.012
581 Seyoum DS, Vojinovic Z, Price RK, Weesakul S. (2012). Coupled 1D and noninertial 2D flood
582 inundation model for simulation of urban flooding. Journal of Hydraulic Engineering 138(1):
583 23–34. https://doi.org/10.1061/(ASCE)HY.1943-7900.0000485
584 Strelkoff, T. S., Tamimi, A. H., and Clemmens, A. J. (2003). Two-dimensional basin flow with
585 irregular bottom configuration. J. Irrig. Drain. Eng., 129(6), 391–401.
586 https://doi.org/10.1061/(ASCE)0733-9437(2003)129:6(391)

587 TavakoliFar, H., Abbasi Zadeh, H., Nazif, S. and Ghasemi, S. (2021). Development of 1D–2D
588 Urban Flood Simulation Model Based on Modified Cellular Automata Approach. JOURNAL OF
589 HYDROLOGIC ENGINEERING 26, no. 2 (2021): 04020065.
590 https://doi.org/10.1061/(ASCE)HE.1943-5584.0002036

591 Walsh, T. C., C. A. Pomeroy, and S. J. Burian. (2014). Hydrologic Modeling Analysis of a Passive,
592 Residential Rainwater Harvesting Program in an Urbanized, Semi-Arid Watershed. Journal of
593 Hydrology 508: 240–253. https://doi.org/10.1016/j.jhydrol.2013.10.038

Webby RB, Adamson PT, Boland J, Howlett PG, Metcalfe AV and Piantadosi J. (2007). The Mekong-applications of value at risk (VaR) and conditional value at risk (CVaR) simulation to the benefits, costs and consequences of water resources development in a large river basin. Ecol Model 20I:89–96. https://doi.org/10.1016/j.ecolmodel.2006.07.033

Yamout MG, Hatfield K, Romeijn HE. (2007). Comparison of new conditional value-at-risk-based management models for optimal allocation of uncertain water supplies. Water Resour Res 43:W07430. https://doi.org/10.1029/2006WR005210

Yazdi, J., Lee, E. H., and Kim, J. H. (2015). Stochastic multi objective optimization model for urban drainage network rehabilitation. Journal of Water Resources Planning and Management, 141(8), 04014091. https://doi.org/10.1061/(ASCE)WR.1943-5452.0000491

Yazdi, J., Torshizi, A.D. & Zahraie. (2016). Risk based optimal design of detention dams considering uncertain inflows. Stoch Environ Res Risk Assess 30, 1457–1471. https://doi.org/10.1007/s00477-015-1171-9

Zhang S, Pan B. (2014). An urban storm-inundation simulation method based on GIS. Journal of Hydrology 517: 260–26. https://doi.org/10.1016/j.jhydrol.2014.05.044

Figures

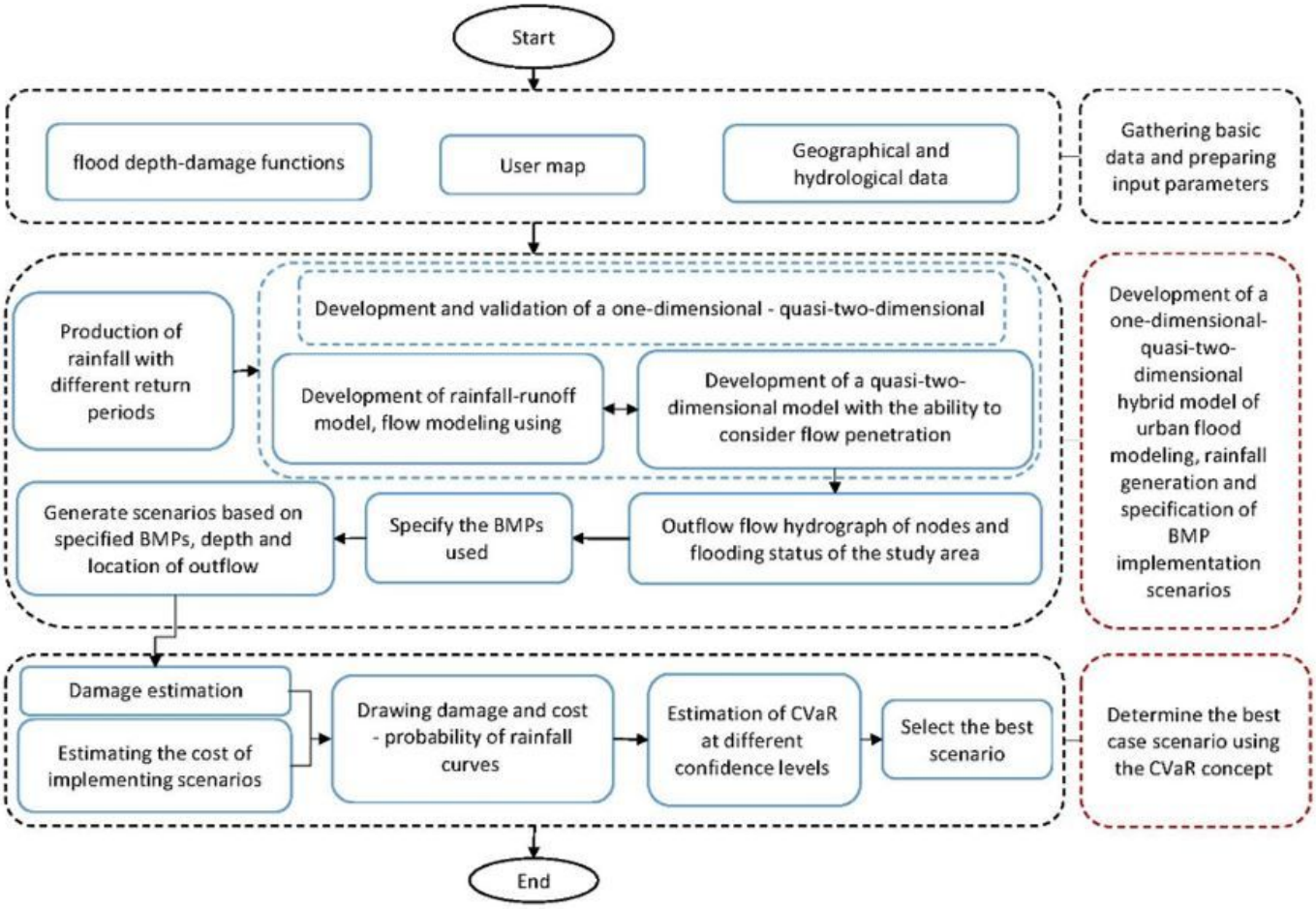

Figure 1

The proposed flood management algorithm with the aim of reducing the damage and cost using the concept of CVaR

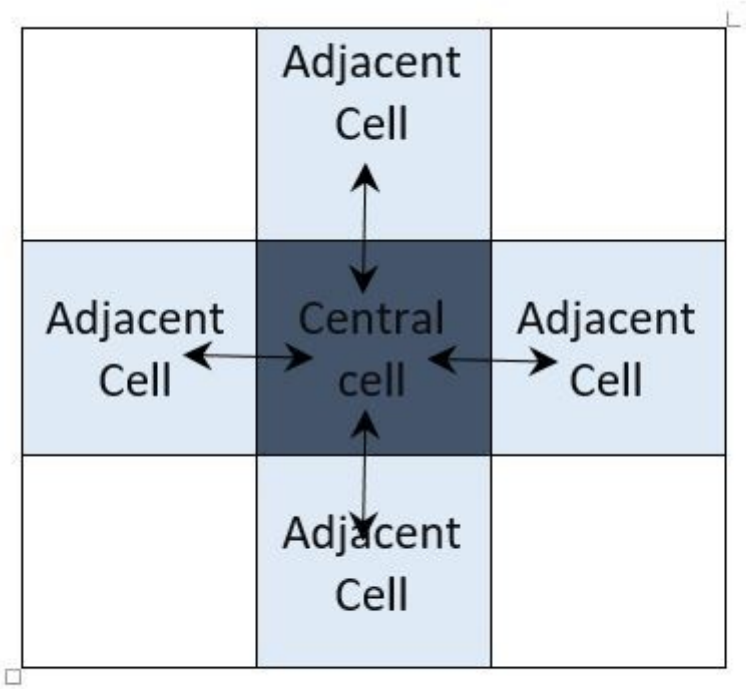

Figure 2

The use of von Neumann neighborhood method to connect the cells

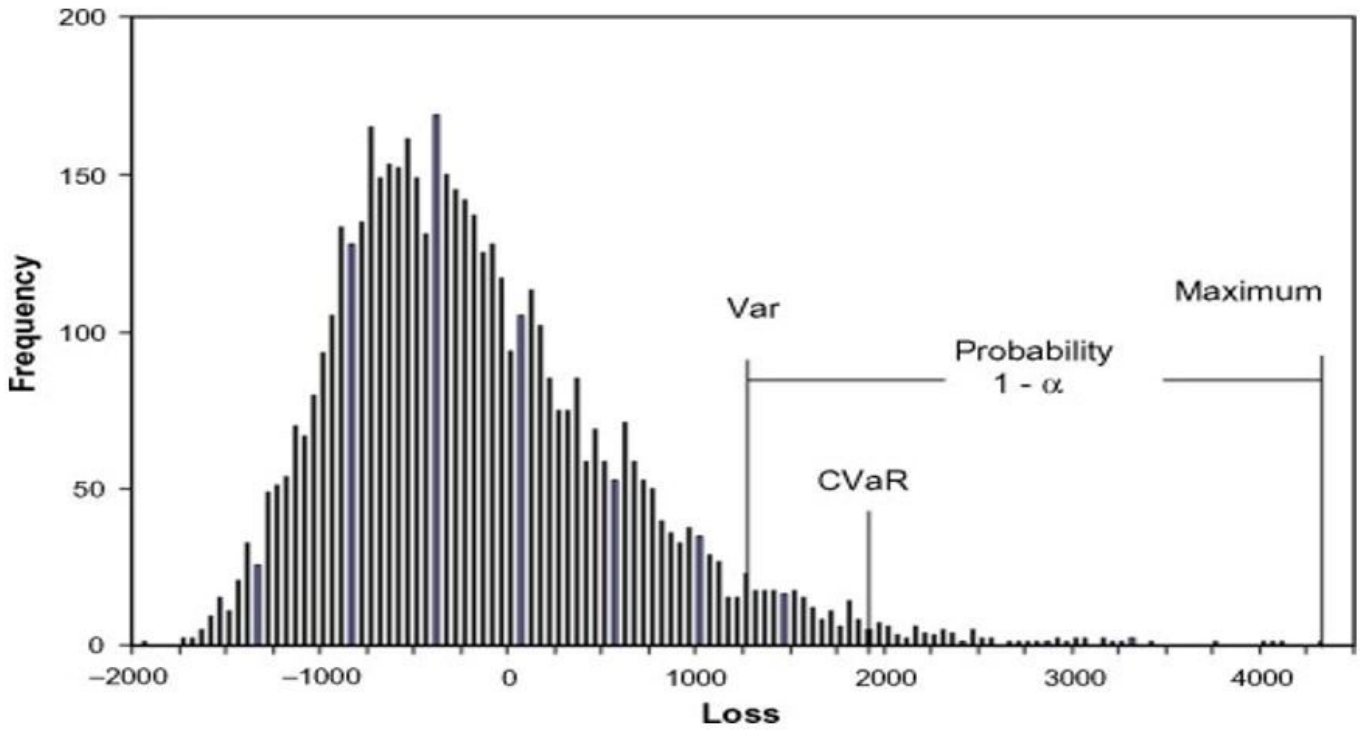

Figure 3

VaR and CVaR descriptions using damage probability density function (Rockafellar and Uryasev, 1999)

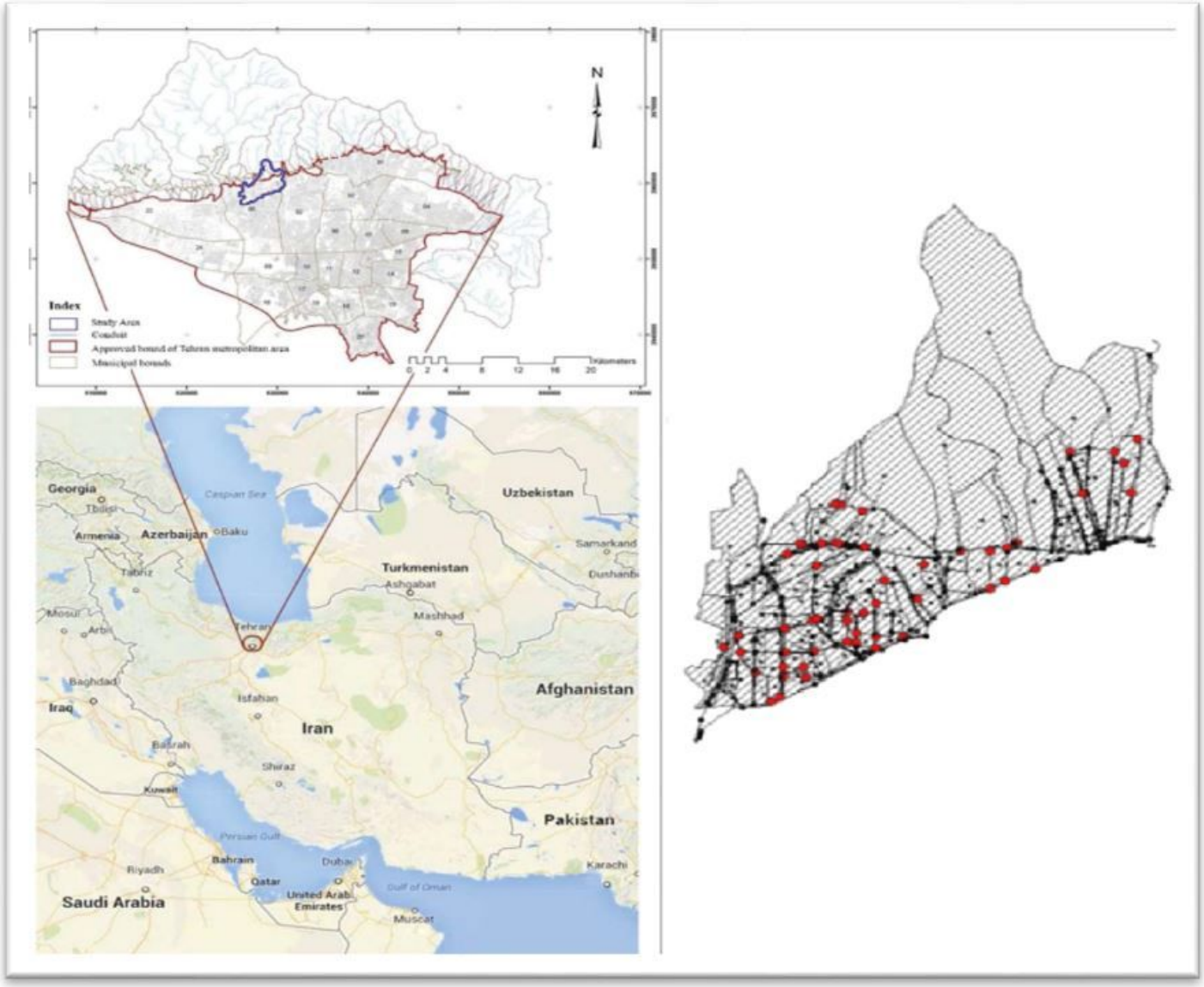

Figure 4

Location of the study area and general outline of the surface water harvesting network along with sub-catchments in the SWMM program

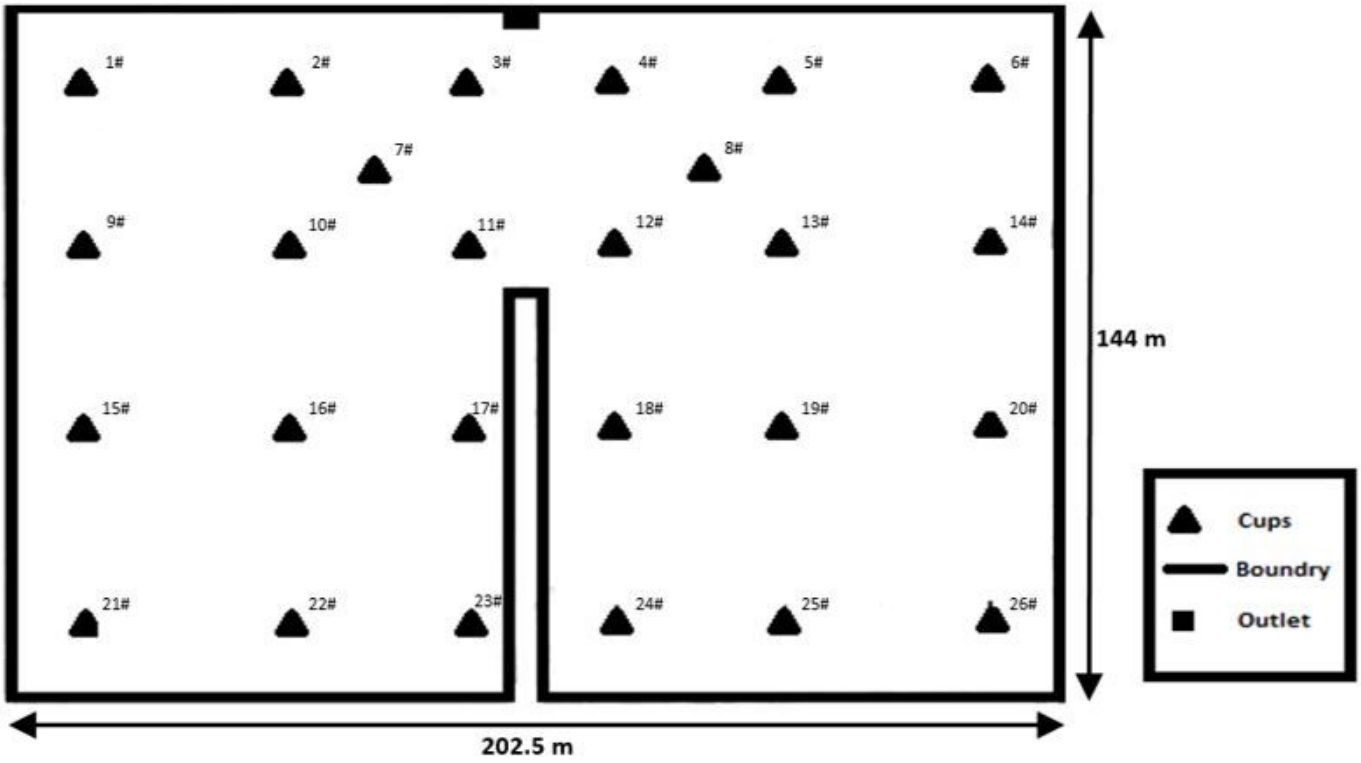

Figure 5

Layout for 2.9 ha Field

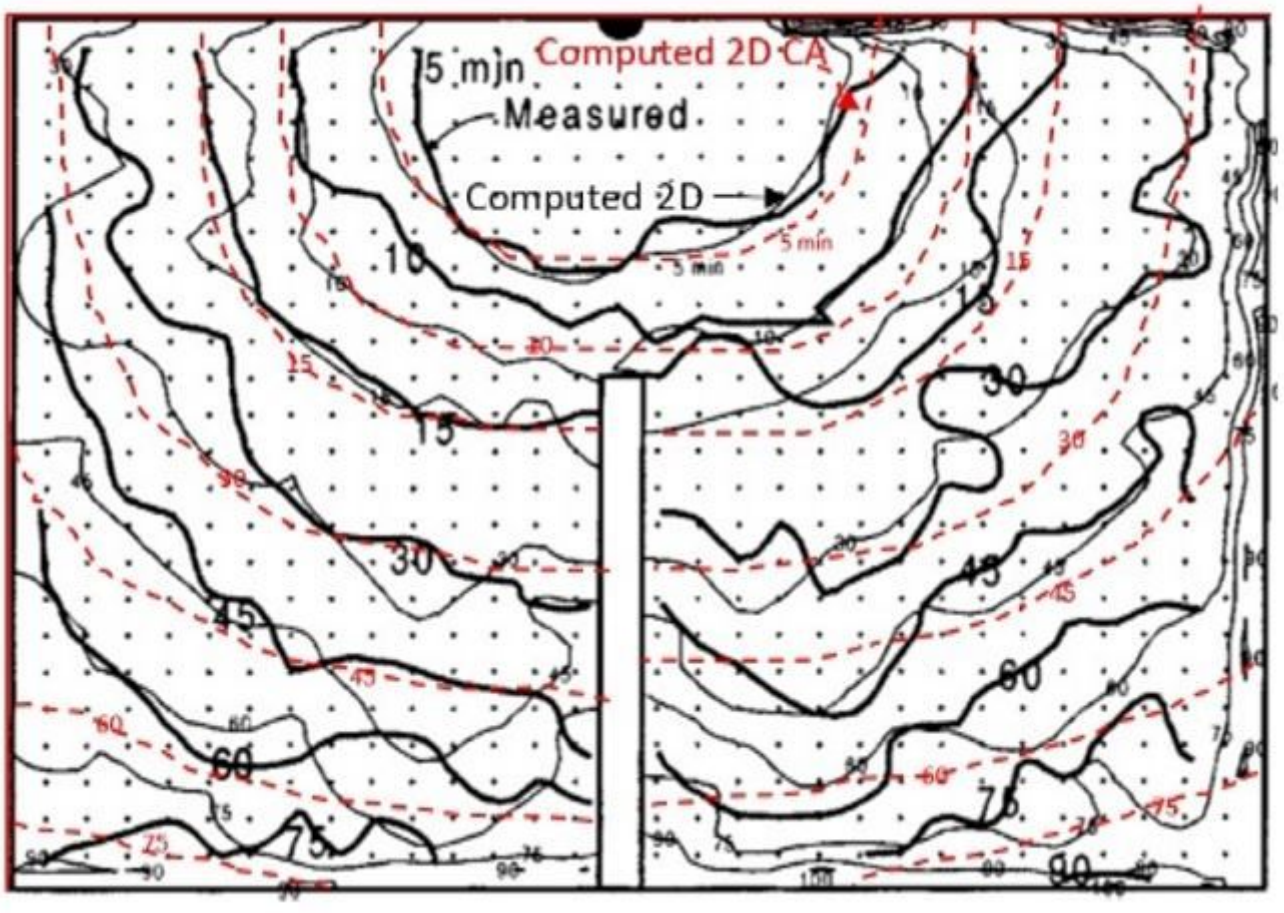

Figure 6

Flow intrusion lines associated with the field measurement, flow modeling conducted by Clemmens et al. (2003) and flow modeling using quasi-2D CA model

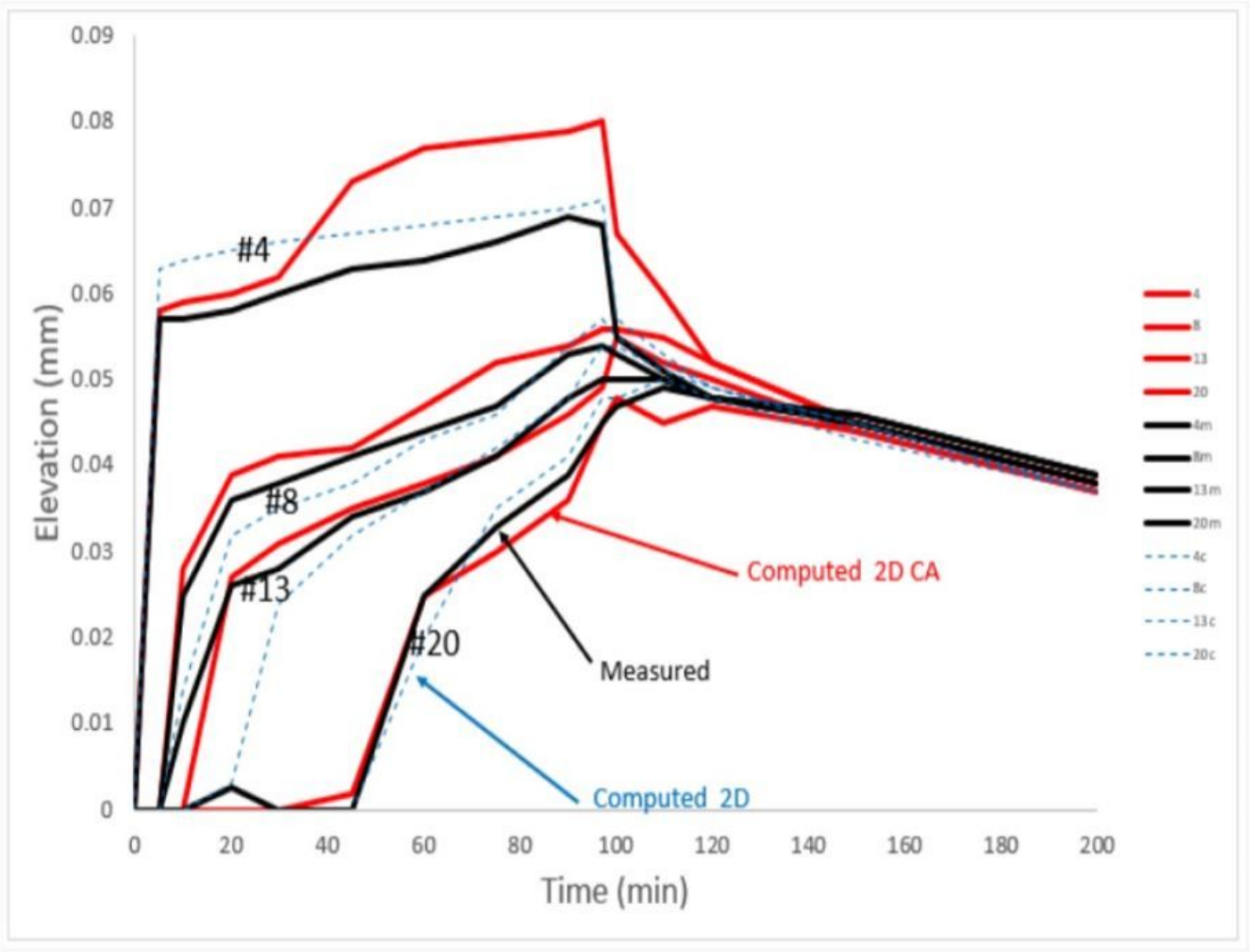

Figure 7

Flow hydrographs at points 4, 8, 13 and 20

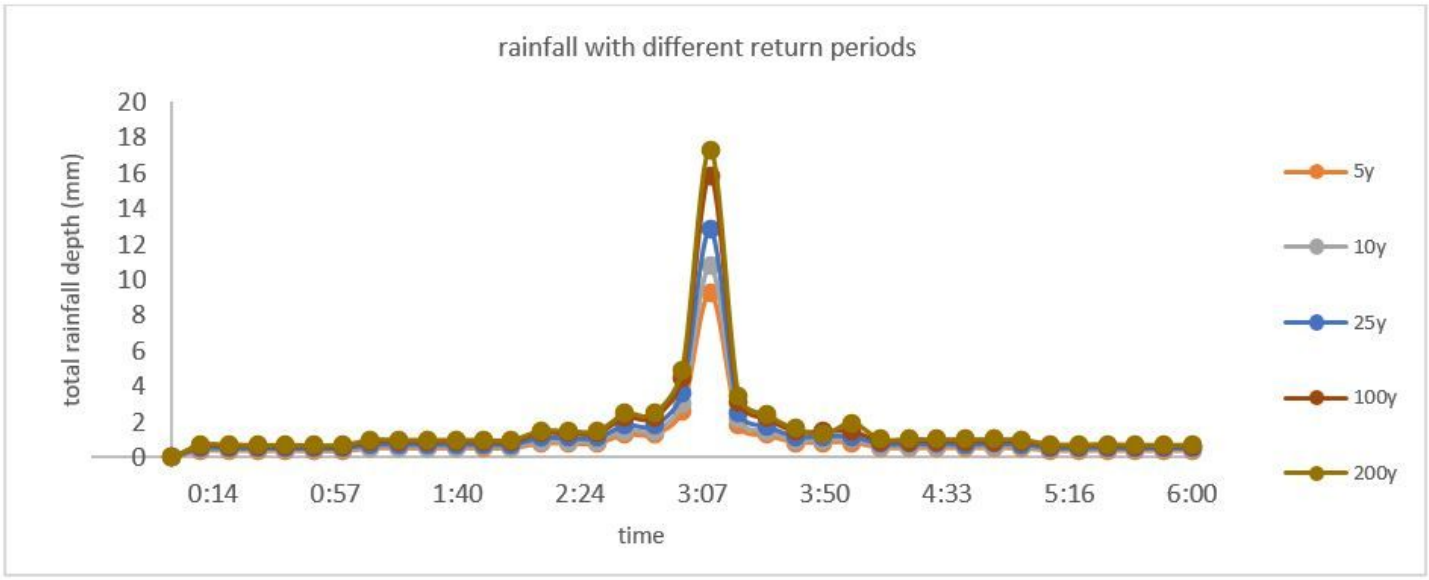

Figure 8

Design rainfall with different return periods for the study area

Figure 9

Node flooding for (a) 10-year and (b) 100-year return periods

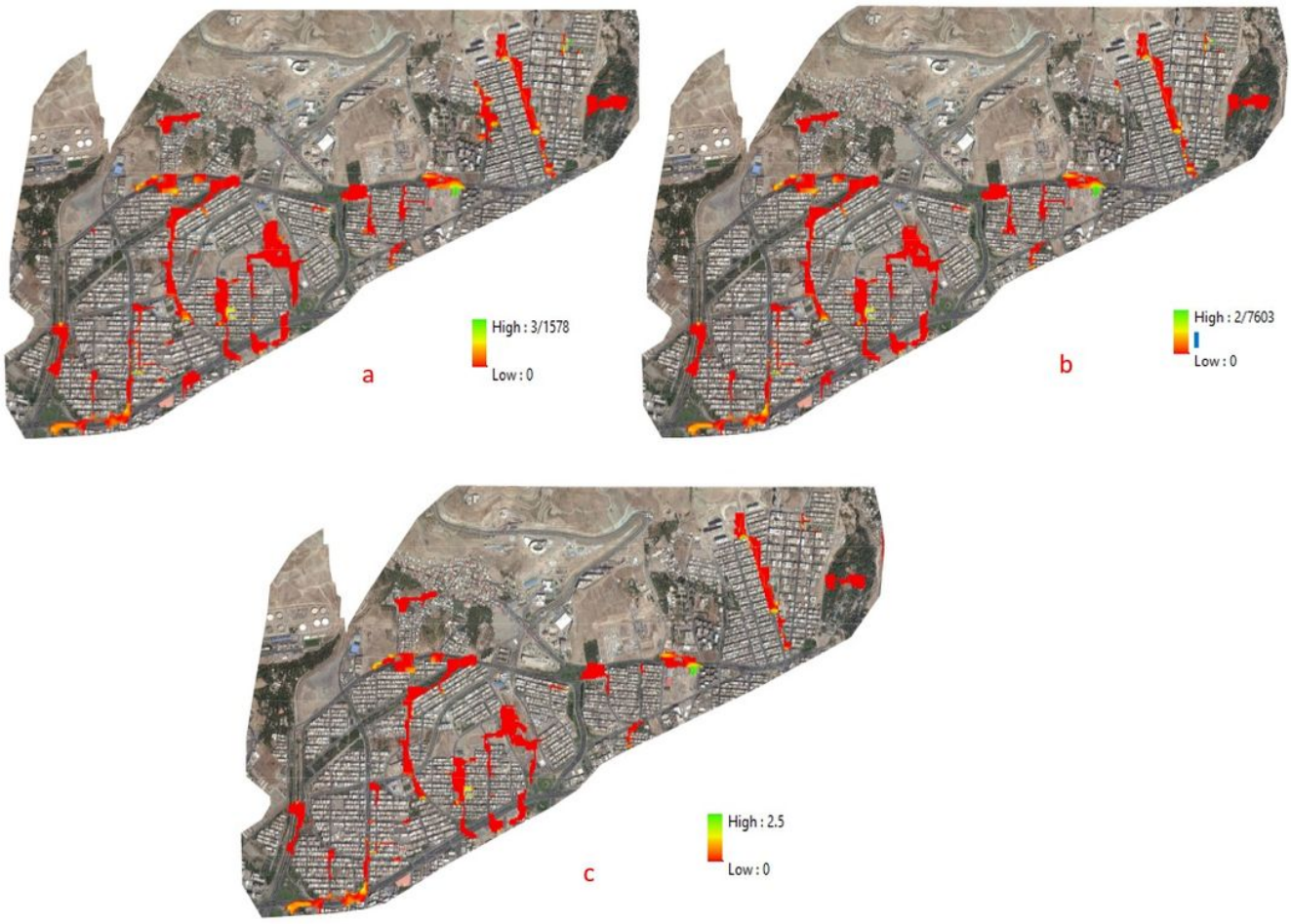

Figure 10

The modeled flooding range and depth associated with (a) 200-, (b) 100- and (c) 50-year return periods

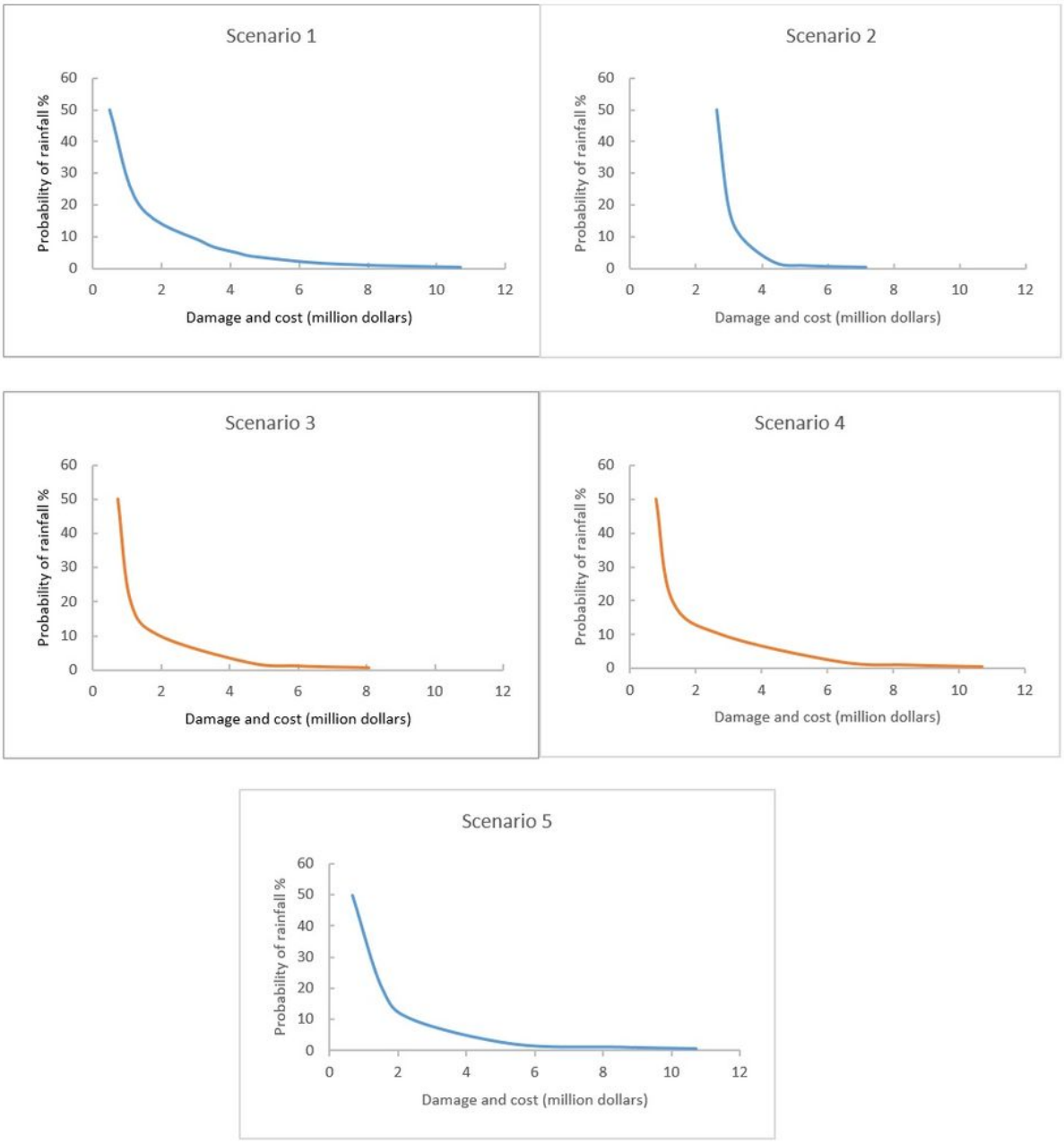

Figure 11

Damage versus probability for different scenarios

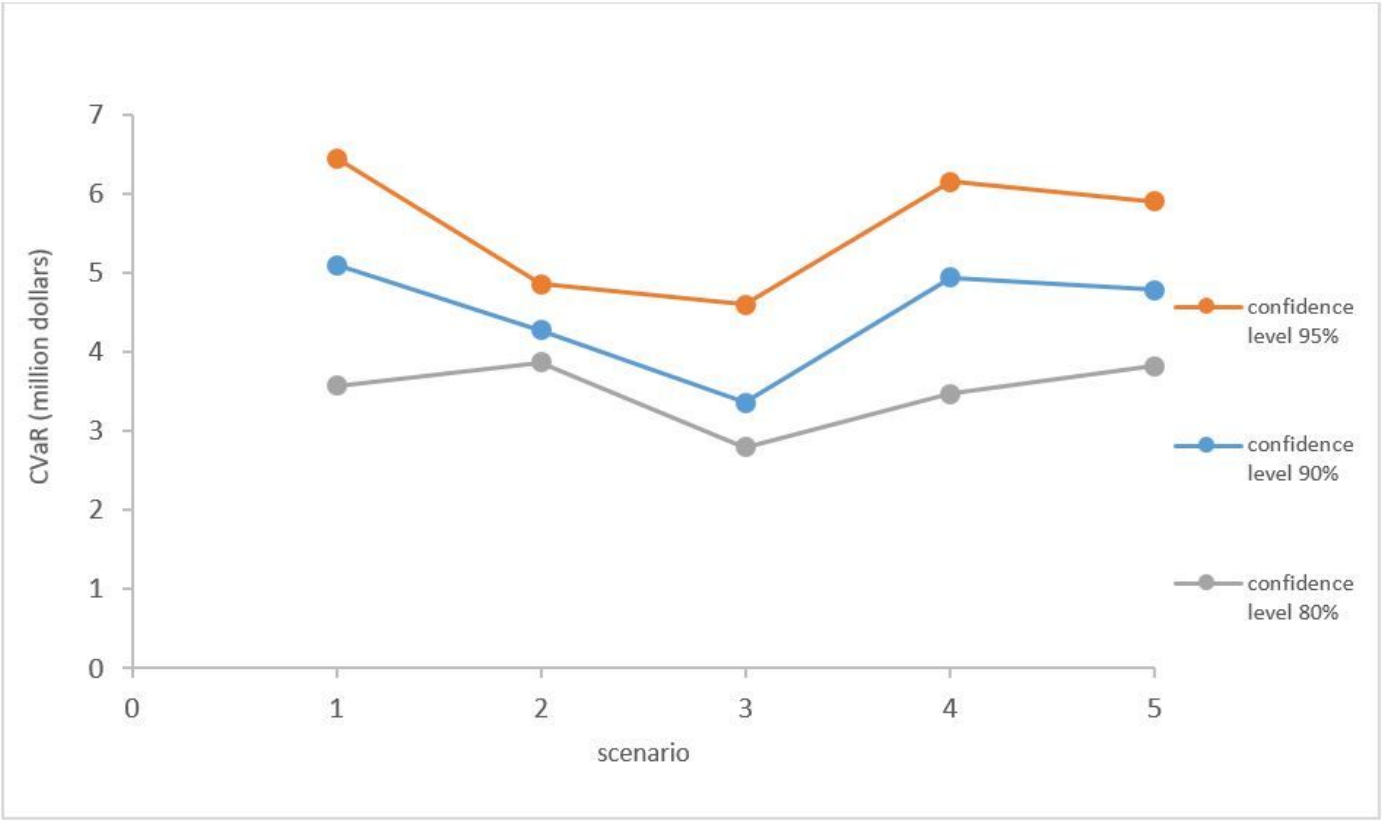

Figure 12

CVaR values at different confidence levels for various scenarios